IET Microwaves, Antennas & Propagation

Research Article

IET Journals
The Institution of Engineering and Technology

Small form factor UWB antenna integrating geopolymer dielectric material

ISSN 1751-8725
Received on 11th September 2018
Revised 11th June 2019
Accepted on 13th June 2019
E-First on 15th July 2019
doi: 10.1049/iet-map.2018.5776
www.ietdl.org

Houda Nadir[1] ✉, Ameni Gharzouni[2], Edson Martinod[1], Noel Feix[1], Olivier Tantot[1], Valerie Bertrand[3], Sylvie Rossignol[2], Michele Lalande[1]

[1]*XLIM, University of Limoges, Brive, France*
[2]*CISTEME, Brive, France*
[3]*SPCTS, University of Limoges, Limoges, France*
✉ *E-mail: edson.martinod@xlim.fr*

Abstract: This study presents a new design of a reduced volumetric ultra-wideband (UWB) antenna using innovative dielectric based on the use of geopolymer material which is safe and eco-friendly. The created antenna is intended to radiate in the air. The impedance mismatch due to interface dielectric/air at the aperture of the antenna imposes to choose dielectric material with an appropriate permittivity value. In this study, the authors focus on the experimental protocol that they use to elaborate a dielectric material with suitable dielectric properties over an UWB domain. An experimental phase of dielectric properties assessment is also described. The conceived antenna is inspired by K-antenna which constitutes the starting point of the proposed new antenna design, particularly because of their small dimensions. The antenna is intended to operate in a frequency band ranging from 300 MHz to 3 GHz. The authors demonstrate that the use of an appropriate innovative dielectric material like a geopolymer is an efficient way to reduce the antenna size. Furthermore, the behaviour of the antenna filled with geopolymer is validated using experimental results.

1 Introduction

For most of the military, civil and medical imaging systems, the ultra-wideband (UWB) antenna is expected to provide very high resolution, which demands an appropriate antenna design. Moreover, the reduction of UWB antenna dimensions for radar applications is rather a difficult task, especially at low frequencies.

Electromagnetic radiation covering a very wide band of frequencies, typically a decade, is usually used in radar systems for the localisation of buried objects in the ground (ground penetrating radar, GPR) [1], or detection behind a partition wall. The resolution of the radar is related to the covered frequency band and its ability to penetrate the investigated medium depends on the radiated frequencies. The performances are better when the radiated band is large and the low frequencies of the spectrum have a low value. Since the dimensions of the radiating element are proportional to the highest radiated wavelength, it is still necessary to find a compromise between the radar resolution and the overall size of the system.

On the other hand, waves propagation in a lossy medium (e.g. walls, grounds) show an attenuation that must be compensated by an appropriate radiation level, by using volumetric antennas rather than planar.

Since 1998, the impulse UWB stands out among the most promising technologies to respond positively to this problem, the advantages of systems using UWB technology over narrowband are undeniable. For example, for electromagnetic detection, systems operating with a single frequency make it possible to optimise different elements of a radar at this frequency so that the efficiency increases, except that the presence of certain obstacles may affect the signal propagation and hinder any detection. It is for this reason that the UWB is a good candidate to solve this kind of problem. Its ability to radiate a wide band of given frequencies allows the detection through obstacles, leading to his frequent use in GPR systems where it showed great interest.

For instance, we contributed to the design of a radar system installed on tunnel boring machine (TBM) which must be able to identify the large obstacles which could interrupt digging operation (e.g. other tunnels, cavities, boulders, foundations, archaeological remains etc.) and the changes in soil conditions (e.g. from sand to gravel) (NETTUN Project) [2]. This radar system must radiate at low frequencies in order to obtain a better penetration into the soil, ideally a few decades of megahertz. Among various antenna designs existing in the literature, K-antenna [3] provides reduced antenna dimensions and high efficiency, which is highly crucial for radar applications. The K-antenna is a combination of an electric-type radiator made as TEM horn and a magnetic loop. It has been chosen as the basic structure for the designed antenna.

There are several ways to reduce UWB antenna dimensions [4–7]. In this work, we focused on the following three techniques dedicated to volumetric antennas:

(i) The first one utilises the concept of loading the appropriate dielectric material [8–10] inside the antenna such that main dimensions of the antenna are divided by the square root value of the dielectric permittivity (ε'_r) of the used material.

(ii) The second technique uses the effective combination of the radiation provided by the electric dipole and a magnetic loop [11]; the same principle is used for K-antenna design.

(iii) The last technique employs resistive elements (resistors). However, the drawback of this technique is low efficiency at low frequencies operations [12–14].

In this work, the dimensions of the designed antenna are reduced using the aforementioned methods, which leads to two-phased design process. In the first phase, the *A*ntenna combines *H*ybrid radiation (electric and magnetic) and the use of *D*ielectric materials. Hereafter, we refer this antenna design as *D*ielectric *H*ybrid *A*ntenna (DHA*)*. In the second phase, the *A*ntenna is integrated inside a cavity, and associates the use of *R*esistive loads at the aperture and *D*ielectric materials. This one is referred as *D*ielectric *R*esistive *A*ntenna (DRA).

In the context of the NETTUN Project, an UWB antenna filled with resin ($\varepsilon'_r = 3.8$ at 1.5 GHz) has been designed. The use of the resin creates exothermic reaction, which can damage the RF connector.

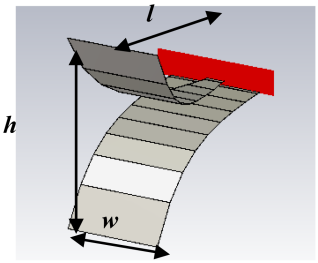

Fig. 1 *Example of progressive wave antenna (unbalanced horn antenna)*

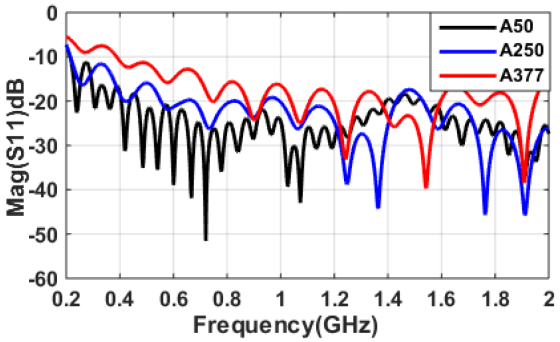

Fig. 2 *Reflection parameters for different characteristic impedance evolution*

In order to eliminate this problem, we propose an innovative dielectric material (geopolymer) [15] to fill the antenna under ambient conditions. Moreover, we establish an efficient control over the proposed dielectric material fabrication and therefore, the effective dielectric permittivity value of the material can be easily obtained in the range of 3.5–10 at 1.5 GHz.

This paper is organised as follows: Section 2 briefly describes the principle and the methodology used for designing progressive wave antennas. The design method of K-antenna and results obtained by CST Microwave Studio are described. Section 3 presents the two design phases (DHA and DRA) of the elaborated antenna and the corresponding theoretical performances. Sectiosn 4 and 5 describe the material fabrication process and the method used for characterising the dielectric material. The fabricated DRA antenna and the experimentally measured antenna performances are presented in Section 6. Finally, Section 8 concludes the paper.

2 Design methodology

2.1 Principle of designing progressive wave antenna

The progressive wave antenna (Fig. 1) radiates waves gradually and in particular, higher frequencies before the lower ones. It can be considered as a cascade of several propagation line sections in which width (w) and height (h) are determined based on the selected characteristic impedance Z, on the dielectric permittivity of the substrate and on the frequencies of the spectrum to be radiated.

For the design of progressive wave antennas, a tool on MATLAB has been developed. It makes it possible to construct the antenna geometry in several sections relying on the standard DRA microstrip line equations [16].

The dimensions of each section 'w' and 'h' are calculated according to the input parameters criteria: $h_0 = \lambda_{min}/10$ (height of the feed), $h \leq \lambda_{max}$ (height of the aperture), $l \leq \lambda_{max}$ (length of the antenna), Z_0 is the input impedance and Z_{max} is the characteristic impedance at the aperture.

For validating the evolution of characteristic impedances from Z_0 to Z_{max} for our proposed antenna design, basic horn antennas have been designed by selecting several choices of Z_{max} values. The horn antennas are designed to operate in the air medium ($\varepsilon'_r = 1$) over the frequency bandwidth from 200 MHz to 2 GHz. The length (l) and the aperture (h) of the antennas are limited by $\lambda_{max}/2$

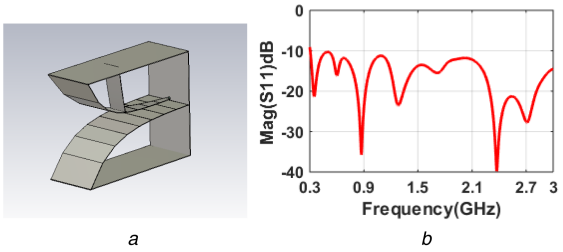

Fig. 3 *K antenna (a) Reflection parameter of K antenna (b)*

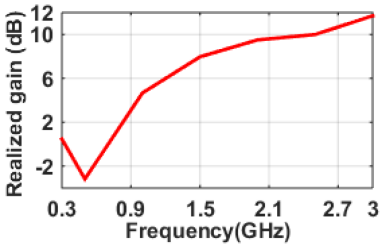

Fig. 4 *Realised gain along the axis of the K antenna*

of the spectrum (Fig. 1). The following three cases have been considered for the design of horn antennas:

i. 50 Ω (A50)
ii. 50–250 Ω (A250)
iii. 50–377 Ω (A377)

If the steady 50 Ω characteristic impedance would be selected for the design, it would lead to a too large antenna dimensions ($W_{max} > \lambda_{max}$) unlike the other two cases. The impedance evolution from 50 to 250 Ω is considered as the best for providing reduced antenna dimensions and suitable adaptation (Fig. 2).

2.2 Application of the design principle on K antenna

To obtain the K antenna as shown in Fig. 3, the structure of unbalanced horn antenna is modified by adding vertical plate at the back and horizontal plates.

K antenna is a combination of electrical and magnetic dipoles, which helps to reduce the antenna dimensions to at least $\lambda_{max}/3.75$. It has been demonstrated that the integration of the magnetic loop on the K antenna allows to enhance the low frequency behaviour of the antenna and also to minimise the reactive energy caused by the imaginary part of its input impedance [17–19]. This would significantly help to increase the antenna directivity and to ensure good impedance adaptation over the desired frequency band of operation.

In this work, the design of the DHA antenna is inspired by the K antenna design principle [20]. For this particular reason, a K antenna design has been first realised (Fig. 3*a*) for the frequency band of 0.3–3 GHz. The respective dimensions of the K antenna are as follows:

$$l = \frac{\lambda_{max}}{3.75} = 26.6\,\text{cm},\ h = \frac{\lambda_{max}}{5} = 20\,\text{cm},\ w = \frac{\lambda_{max}}{10} = 10\,\text{cm} \quad (1)$$

The antenna shows a good matching (Fig. 3*b*) and a maximum gain of 12 dB (Fig. 4) is obtained.

3 Design process of DRA antenna design

3.1 First design phase: DHA antenna

The DHA antenna (Fig. 5) design uses the combination of hybrid dipole (electric and magnetic) and an appropriate dielectric material. The chosen frequency band for the design is 0.3–3 GHz and it is intended to radiate in the air medium.

For this study, CST Microwave Studio software has been used for the antenna simulation and for defining the dielectric characteristics of the material by using a first-order Debye model

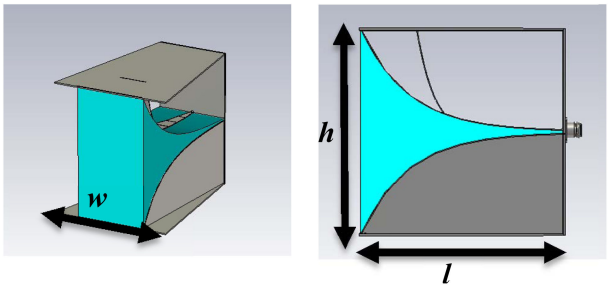

Fig. 5 *DHA antenna*

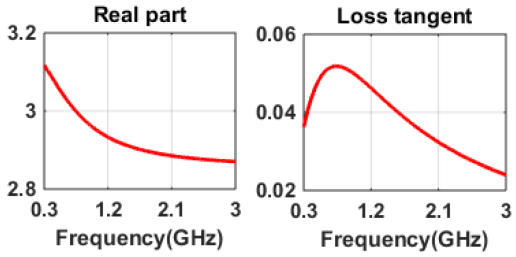

Fig. 6 *Dielectric characteristics introduced in CST*

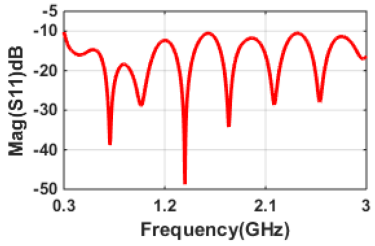

Fig. 7 *Reflection parameter of DHA antenna*

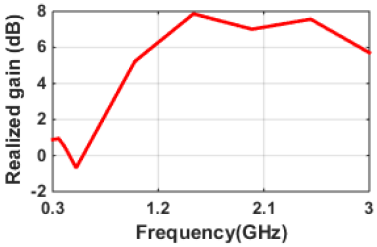

Fig. 8 *Realised gain along the axis of the DHA antenna*

[21] (Fig. 6). The antenna has been partially filled with dielectric material whose permittivity $\varepsilon'_r = 3$ and the loss tangent $\tan\delta = 0.03$ at 1.5 GHz. This specific value of ε'_r has been selected in order to minimise the reflection between the interface of dielectric/air at the antenna's aperture and to obtain smooth propagation of waves to the air medium.

Furthermore, the value of the loss tangent has been chosen to lead to the common dielectric properties value of the geopolymer, which will fill our antenna.

The DHA antenna dimensions and the characteristic impedance are optimised and calculated in function of the average dielectric permittivity value of the air and the dielectric material $\left(\varepsilon_e = \frac{\varepsilon'_r + \varepsilon_{air}}{2}\right)$. The DHA impedance evolution which has been applied evolves from 50–250 Ω/ $\sqrt{\varepsilon_e}$.

$$l = \frac{\lambda_{max}}{4.5} = 22\,\text{cm},\ h = \frac{\lambda_{max}}{5} = 20\,\text{cm},\ w = \frac{\lambda_{max}}{5.5} = 18.1\,\text{cm} \quad (2)$$

The simulated antenna performances are given in Figs. 7–9. A good matching ($S_{11} < -10$ dB) is observed over the frequency bandwidth of 0.3–3 GHz and a maximum gain of 7.5 dB is obtained (Fig. 8).

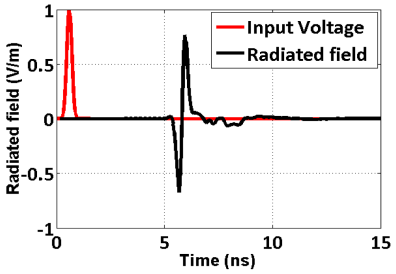

Fig. 9 *Radiated field of DHA antenna*

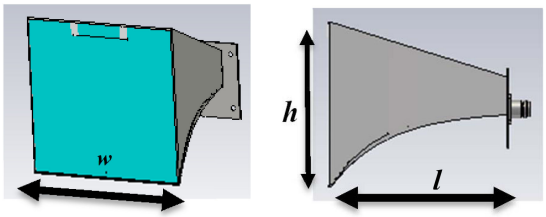

Fig. 10 *DRA antenna*

The radiated field of simulated DHA antenna (Fig. 9) is calculated 1 m from the antenna's aperture, for the applied input voltage of 1 V. The magnitude of the radiated peak-to-peak field for the DHA antenna is 1.43 V for a group delay of 0.14 ns. The group delay is calculated using the following equation [22], this low value of group delay shows that this antenna is not too dispersive:

$$\tau_g\text{rms} = \sqrt{\frac{1}{\Delta f}\int_{f_1}^{f_2}(\tau_g - \overline{\tau_g})^2 df} \quad (3)$$

With $\tau_g(f) = -\frac{\partial\varphi}{2\pi\partial f}$ and $\overline{\tau_g} = \frac{1}{\Delta f}\int_{f_1}^{f_2}\tau_g df = -\frac{\Delta\varphi}{2\pi\Delta f}$,

$\Delta f = f_2 - f_1$

where:

φ is the phase of transfer function for given polarisation.

f_1 and f_2 the lower and the higher frequency, respectively, of the operation bandwidth.

The DHA antenna size remains significant comparing to K antenna dimensions. The optimum size reduction would be obtained by dividing the dimensions by $\sqrt{\varepsilon_r}$, this implies that the antenna must be completely immersed into a dielectric material. To ensure this, the propagation medium need to be limited by a cavity of finite dimensions. A parametric study has been realised to determine the optimum cavity size.

3.2 Final design phase: DRA antenna design and performances

In order to design the DRA antenna (Fig. 10), the antenna is integrated into a metallic cavity. The frequency band of 0.3–3 GHz is considered and it is intended to radiate in the air medium. The antenna has been completely filled with dielectric material shown in Fig. 6 ($\varepsilon'_r = 3$, $\tan\delta = 0.03$ at 1.5 GHz). The corresponding antenna design is shown in Fig. 10. However, the cavity disturbs the radiation of the low frequencies; Indeed, below 500 MHz, the waves cannot be radiated because of the cavity effect. For the lower frequencies, the antenna dimensions are not sufficient to allow a good radiation; the antenna behaves as a cable extension. This problem can be solved by matching to 50 Ω (the characteristic impedance of the feeder cable) the end of the transmission line by using four 200 Ω resistors placed at the aperture. For the higher frequencies, the sidewalls influence is negligible because the waves are radiated closer to the feeder and the corresponding current cannot reach the end of the antenna. The respective dimensions of

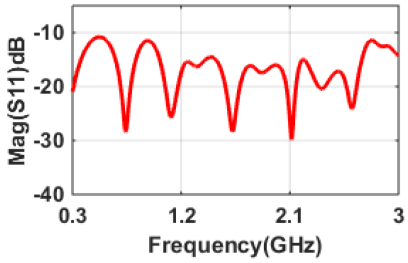

Fig. 11 *Reflection parameter of DRA antenna*

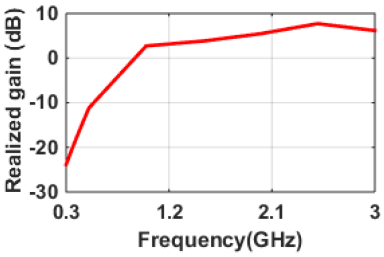

Fig. 12 *Realised gain along the axis of the DRA antenna*

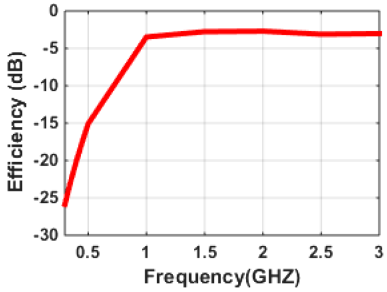

Fig. 13 *Theoretical total efficiency of DRA antenna over frequency band*

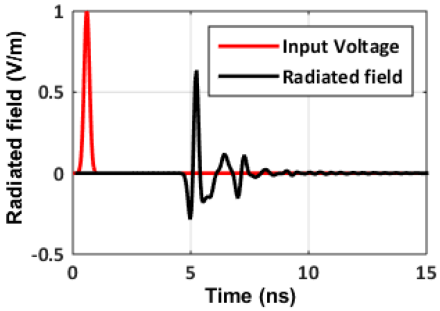

Fig. 14 *Radiated field of DRA antenna*

the DRA antenna after optimisation via CST Microwave Studio are as follows:

$$l = \frac{\lambda_{max}}{6.5} = 15.3\,\text{cm},\ h = \frac{\lambda_{max}}{7} = 14.2\,\text{cm},\ w = \frac{\lambda_{max}}{5.8} = 17.2\,\text{cm} \quad (4)$$

The antenna shows very good reflection parameter (Fig. 11) over the desired frequency band and a maximum gain of 9 dB (Fig. 12) is obtained. However, the drawback of this antenna is low gain at low frequencies due to the presence of resistors in the design.

Fig. 13 shows the theoretical antenna efficiency over the frequency band. The DRA antenna efficiency is low below 500 MHz. The gain and efficiency values at low frequencies are low because of using resistors and the antenna size particularly at the aperture.

The magnitude of the radiated peak-to-peak field for the DRA antenna (Fig. 14) is 0.91 V for a group delay of 0.43 ns; it is calculated 1 m from the antenna's aperture, for the applied input voltage of 1 V. The group delay is higher than for DHA antenna

Table 1 Comparison of K and DRA antennas characteristics

Antenna	Frequency band	Dimensions, cm (L × H × W)	Maximum gain, dB
K	0.3–3 GHz	26.6 × 20 × 10	12
DRA	0.3–3 GHz	15.3 × 14.2 × 17.2	9.0

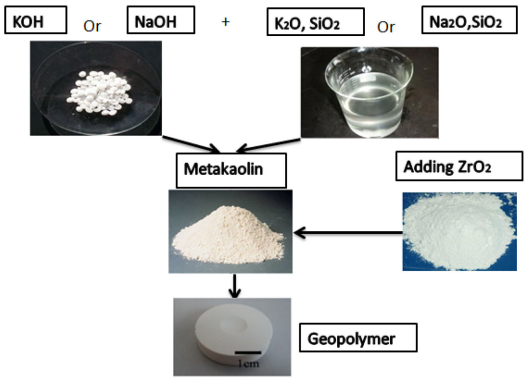

Fig. 15 *Experimental process for obtaining geopolymer material*

which could be a drawback for a GPR application. However, this final design phase yields to decrease the antenna size.

Table 1 shows a comparison between the dimensions and the gain of K antenna (the starting point) and the final design of DRA antenna for the same frequency bandwidth.

It can be seen from Table 1 that in spite of lower maximum gain value, DRA antenna design offers reduced antenna dimensions. The antenna has smaller dimensions (L and H), thus it has a slightly lower gain level, but the main problem in reducing the overall size of a UWB antenna has been achieved. Moreover, in addition to the fact that we used two antenna reduction techniques, the novelty is linked to the fact that we associate a geopolymer material (Section 4.) to an electromagnetic context with this antenna design. For this reason, we have manufactured this particular antenna. The corresponding design and the measurement results are presented in Sections 5 and 6.

4 Scope of fabricating the new innovative material

4.1 Geopolymer material

Today, it is becoming increasingly important to develop materials that are safe and eco-friendly such as geopolymer. It is an inorganic aluminosilicate material. It does not contain any solvents and therefore, it will not burn and emit any gas or toxic fumes. Similar to rock, it is resistant to chemical aggression and erosion. The raw materials involved are mainly minerals according to the geological origin.

The significance of fabricating geopolymer material for the antenna applications is to control and obtain the desired dielectric permittivity value. This allows the material to be fabricated and then be filled into the antenna at ambient temperature, without neither exothermic reaction nor harmful substances emissions.

4.2 Experimental protocol for obtaining a geopolymer material

To obtain geopolymer material, the potassium hydroxide or sodium hydroxide is added to an alkaline solution. Metakaolin was added to the solution. Moreover, some additives such as ZrO_2 or $BaTiO_3$ are also included to obtain high dielectric permittivity values [23].

The permittivity measurements of different formulations using the experimental process presented in Fig. 15 showed reproducible values ranging from 4 to 10.

These values are too high for our application. In order to obtain geopolymer material with $\varepsilon'_r = 3$ at 1.5 GHz, the ZrO_2 has been omitted and replaced by porogene agent (Al). This use of

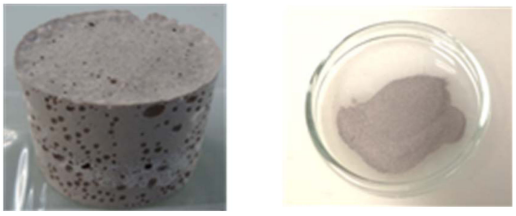

a b

Fig. 16 *Geopolymer sample (a) Mixed with alumina powder (b)*

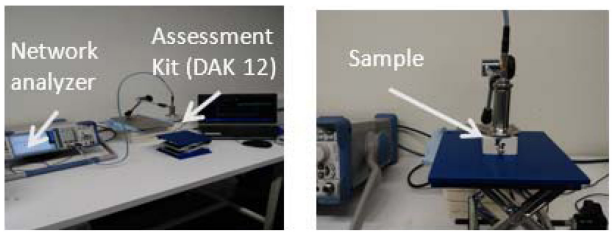

Fig. 17 *Dielectric assessment kit (DAK 12)*

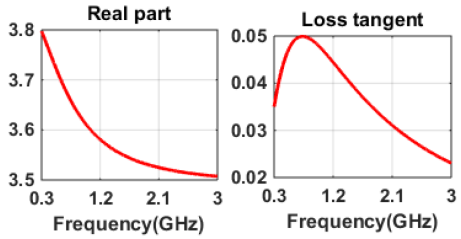

Fig. 18 *Dielectric characteristics of a geopolymer sample*

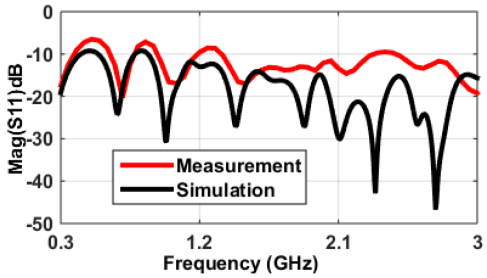

Fig. 19 *Measured and simulated adaptation parameter*

aluminium creates porosity into the material as shown in Fig. 16, and leads to decrease the permittivity value. The pores diameters are between 1 and 3 mm.

4.3 Material characterisation

The dielectric material measurements were approved using the Kit DAK-12 (Fig. 17) [24] product line from Schmidt & Partner Engineering AG (SPEAG), which gives high-precision dielectric parameter measurements (permittivity, conductivity, and loss tangent) over the frequency range from 10 MHz to 3 GHz. The probe is connected using a cable to a vector network analyser (VNA), which is then calibrated with open, short and a liquid with well-known parameters (saline water, concentration: 0,1 mol/l). Dielectric probe is used to measure the dielectric parameters of material over a wide frequency range. The complex permittivity $\varepsilon_r = (\varepsilon'/\varepsilon_0) - j(\varepsilon''/\varepsilon_0)$ (ε': real relative permittivity, ε'': imaginary relative permittivity where $\varepsilon_0 = 8.854$ pF/m is the permittivity in free space) is determined from the measured S_{11} parameter using the VNA and specific software dedicated to the DAK-12. The probe is a cut off section of 50 Ω transmission line used for contact measurement. The samples are measured either by touching the probe to the surface of a solid or by immersing it into a liquid medium. The error of the dielectric measurement is estimated to be 2% for permittivity and 3% for loss tangent.

Fig. 20 *DRA antenna without geopolymer and resistive loads*

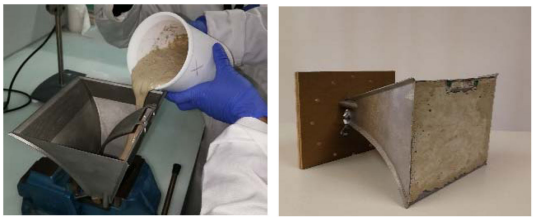

Fig. 21 *Filled DRA antenna*

Different formulations have been tested in order to obtain permittivity value of 3 at 1.5 GHz. Fig. 18 shows the measured optimum dielectric characteristics ($\varepsilon_r = 3.5$, $\tan\delta = 0.03$ at 1.5 GHz) using the DAK12 probe.

The selected optimal composition (Fig. 18) allows a good mechanical strength (solidity and friability), while maintaining the best possible permittivity value. The corresponding composition is 2/3 (potassium hydroxide + Metakaolin + 0.1% Al) + 1/3 (sodium hydroxide + 0.1% Al).

The obtained characteristics from the preliminary geopolymer sample have been introduced in CST Microwave Studio for the antenna simulation.

The DRA antenna simulation results (Fig. 19) led to the manufacture of a prototype.

5 Antenna fabrication and filling

The antenna has been manufactured (Fig. 20) with a 3D printer using 316L stainless steel by the SLM (selective laser melting) process on a Renishaw AM 250 machine.

Firstly, the geopolymer mixture is prepared, and then the obtained liquid is emptied into the antenna at ambient temperature (Fig. 21).

To ensure a homogeneous drying and consolidation of the material, the antenna is filled in three steps, for each one the antenna is put in oven for three days at 90°. The final filled antenna is shown in Fig. 21.

6 Measurements

The S_{11} parameter measurement has been performed on the DRA structure and the comparison between the measured and simulated S_{11} parameters using the optimal dielectric characteristics (Fig. 18) are shown in Fig. 19.

The matching bandwidth strongly depends on the permittivity value, which can explain the difference between the simulation result obtained using $\varepsilon'_r = 3$ at 1.5 GHz (Fig. 11, Section 3.2) and the measurement result with $\varepsilon'_r = 3.5$ at 1.5 GHz.

However, the S_{11} parameter of the fabricated DRA antenna filled with the geopolymer dielectric material is in good agreement with the simulation.

The gain of the DRA antenna integrating geopolymer material is measured and compared with the results of simulations obtained by CST Microwave Studio (Fig. 22). We can see that the results are quite similar.

The E and H plane radiation patterns for frequencies 1, 2 and 3 GHz have been also measured and are shown in Figs. 23–25.

The radiation patterns are consistent with the simulation. It is observed that the measured gain for angles close to $\theta = \pm 180°$ are lower than in simulation, because of the holding system located at the back of the antenna. The observed difference at 3 GHz may be due to the characteristics of the dielectric material that we are not

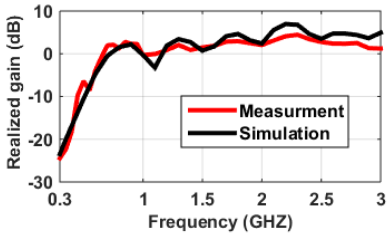

Fig. 22 *Realised gain along the axis of the DRA antenna*

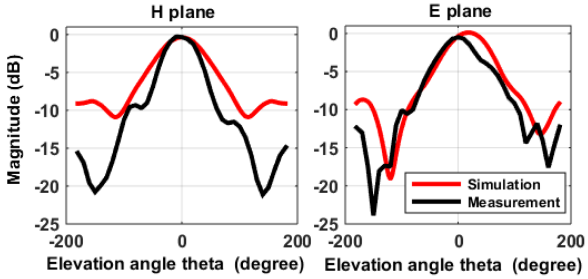

Fig. 23 *Measured and simulated E-plane and H-plane radiation patterns at 1 GHz*

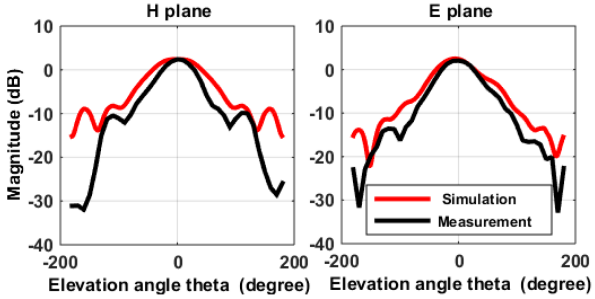

Fig. 24 *Measured and simulated E-plane and H-plane radiation patterns at 2 GHz*

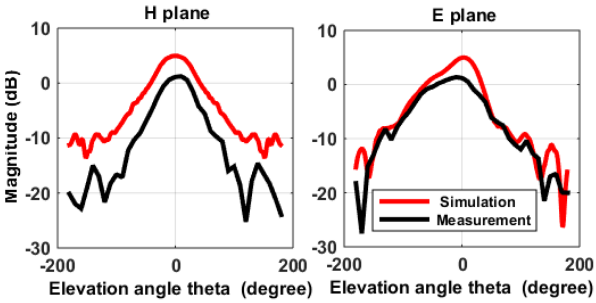

Fig. 25 *Measured and simulated E-plane and H-plane radiation patterns at 3 GHz*

able to characterise once the antennas are filled. This difference is also noted on the figure of the realised gain of the DRA antenna presented in Fig. 22 at 3 GHz. Indeed, the geopolymer inside the antenna may not be totally dry. This hypothesis was confirmed by the results of a new simulation. In order to take into account a material which is not totally dry, we replaced the loss tangent variation (Fig. 18) by $\tan\delta = 0.06$ which matches a classical slightly wet geopolymer. The results on Fig. 26 show that the simulation and the measurement are in good agreement after this modification.

To measure the radiated field, the DRA antenna has been supplied by a pulse delivered by a Kentech APG1 generator. It delivers a Gaussian pulse, with a peak value of 220 V, which covers a spectrum ranging from 0 to 5 GHz at − 20 dB (Fig. 27).

The measured and simulated radiated fields have the same shape, with a peak-to-peak magnitude of 149 V/m in simulation and 122 V/m in measurement (Fig. 28). The difference is probably related to the variation of the value of the real dielectric

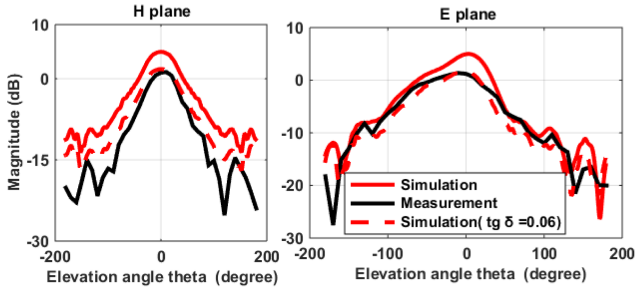

Fig. 26 *Measured and simulated ($\tan\delta = 0.06$) E-plane and H-plane radiation patterns at 3 GHz*

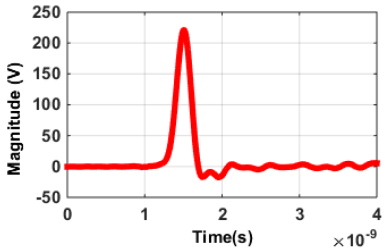

Fig. 27 *Delivered pulse by a Kentech APG1 generator*

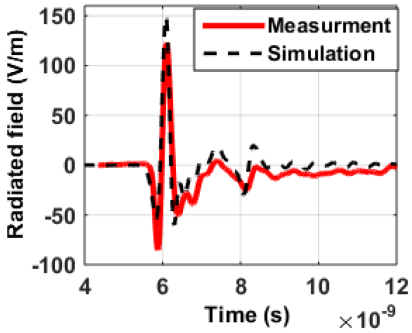

Fig. 28 *Measured and simulated radiated field calculated 1 m from the DRA antenna's aperture*

permittivity inside the antenna, which is not considered in simulation.

7 Reduction size comparison with other techniques

In Table 2, we focus on volumetric antennas on which different kinds of miniaturisation techniques have been applied.

Even if the matching bandwidth and context of use are different, we notice that the DRA antenna offers a good compromise between the maximum gain and the final dimension in relation to the maximum wavelength. However, the drawback is the efficiency of the DRA antenna at low frequencies.

8 Conclusion

In this paper, a new UWB antenna design has been suggested. We have put emphasis on the advantage of using the dielectric material for an UWB antenna design to reduce its dimensions. Moreover, for the first time the contribution of geopolymer material for obtaining the desired dielectric constant value has also been described. The first measurements of the fabricated DRA antenna filled with the geopolymer dielectric material have been performed and found to be in good agreement with the simulation.

On the one hand, the IRCER laboratory keep looking for the suitable formulation to obtain the desired value of $\varepsilon'_r = 3$ and on the other hand actual studies focus on a way to stabilise the humidity rate after the drying procedure by hydrophobic compound adjunction.

In view of the antenna properties, this one can be used for ground penetrating radar application for example. Indeed, the value

Table 2 Comparison of different UWB volumetric antennas after application of a reduction size technique (λ_{max} is the greater wavelength of the matching bandwidth)

Antenna type	Miniaturisation	Matching bandwidth, GHz	Maximum gain	Dimension (L × W × H), cm
3D TEM horn [8]	partially loaded with absorbent material	[0.83–13]	10 dB @ 12 GHz	17.8 × 19.74 × 14 0.49 λ_{max} x 0.54 λ_{max} × 0.39 λ_{max}
dielectric tapered horn Wedge [9]	totally filled with dielectric foam	[1–5]	10 dB @ 5.5 GHz	15 × 15 × 25 1.5 λ_{max} x 1.5 λ_{max} × 2.5 λ_{max}
monocone [25]	multilayer polymer ceramic composite	[2.41–7.98]	3 dB @ 6 GHz	Φ = 5.83 cm; H = 2.915 cm 4.7 λ_{max} × 2.37 λ_{max}
compact Vivaldi TEM horn [26]	Partially loaded + resistive sheet	[1–10]	11 dBi @ 10 GHz (directivity)	9 × 18 × 18 0.9 λ_{max} × 1.8 λ_{max} × 1.8 λ_{max}
compact DRH antenna [27]	partially filled	[0.08–1]	12 dB @ 1 GHz	117 × 70 × 80 0.31 λ_{max} × 0.18 λ_{max} × 0.21 λ_{max}
DRA	fully filled with geopolymer + resistors	[0.3–3]	9 dB @ 3 GHz	15,3 × 14.2 × 17.2 0.15 λ_{max} × 0.142 λ_{max} × 0.17 λ_{max}

of the dielectric permittivity [3, 5–3, 8] allows to use this antenna in front of dielectric value between (1–∼12) without having too much mismatch effect. However this case of application constitutes a novel study. For the next work, the dielectric materials with high dielectric permittivity will be used to further enhance the compactness of the antenna for GPR application.

9 Acknowledgment

We greatly appreciate the 'Region La Nouvelle Aquitaine'.

10 References

[1] Turk, A.S.: 'Ultra-wideband Vivaldi antenna design for multisensor adaptive ground-penetrating impulse radar', *Microw. Opt. Technol. Lett.*, 2006, **48**, (5), p. pp. 834–839

[2] Nadir, H., Sow, M., Négrier, R., *et al.*: 'Design of impulse UWB volumetric antenna integrating dielectric material'. 2016 European Radar Conf. (EuRAD), London, UK, October 2016, pp. 145–148

[3] Andreev, Y.A., Buyanov, Y.I., Koschelev, V.I.: 'Combined antennas for high-power ultrawideband pulse radiation'. Int. Symp. on High-Current Electronics, Tomsk, Russia, 2008

[4] Chen, C.-C., Kramer, B.A., Volakis, J.L.: 'Considerations on size reduction of UWB antennas'. 2007 IEEE Antennas and Propagation Society Int. Symp., Honolulu, HI, 2007, pp. 6011–6014

[5] Ameri, A.A.H., Kompa, G., Bangert, A.: 'Study about TEM horn size reduction for ultrawideband radar application'. 2011 German Microwave Conf., Darmstadt, 2011, pp. 1–4

[6] Kramer, B.A., Chen, C.-C., Volakis, J.L.: 'Size reduction of a low-profile spiral antenna using inductive and dielectric loading', *IEEE Antennas Wirel. Propag. Lett.*, 2008, **7**, pp. 22–25

[7] Li, Y.T., Yang, X.L., Li, Z.B., *et al.*: 'A unidirectional cylindrical conformal monopole antenna designed for impulse radar system', *IEEE Antennas Wirel. Propag. Lett.*, 2011, **10**, pp. 1397–1400

[8] Keskin, A.K., Türk, A.S.: 'Dielectric loaded TEM horn-fed ridged horn antenna design for ultrawideband ground-penetrating impulse radar', *Turk. J. Electr. Eng. Amp Comput. Sci.*, 2015, **23**, (5), p. pp. 1479–1488

[9] Yarovoy, A., Zijderveld, J.: 'Analysis of radiation from a dielectric wedge antenna', in Sabath, F., Mokole, E.L., Schenk, U., *et al.* (Eds): '*Ultra-wideband, short-pulse electromagnetics 7*' (Springer, New York, NY, USA, 2007), pp. 325–333

[10] Demirel, S., Çalişkan, A., Mersin, M.T., *et al.*: 'Design of dielectric lens loaded double ridged horn antenna for millimetre wave application'. 2016 21st Int. Conf. on Microwave, Radar and Wireless Communications (MIKON), Krakow, Poland, May 2016, pp. 1–4

[11] Kim, J.S., Yoon, Y.J., Kwon, H.O., *et al.*: 'A directive subminiature antenna for high-power ultrawideband pulse radiation', *IEEE Antennas Wirel. Propag. Lett.*, 2014, **13**, pp. 1565–1568

[12] Chang, L.-C.T., Burnside, W.D.: 'An ultrawide-bandwidth tapered resistive TEM horn antenna', *IEEE Trans. Antennas Propag.*, 2000, **48**, pp. 1848–1857

[13] Xia, D.Y., EdwDRAs, J.: 'Optimization of UWB pyramidal horn antenna with load'. 2007 Int. Symp. on Microwave, Antenna, Propagation and EMC Technologies for Wireless Communications, Hangzhou, China, August 2007, pp. 673–675

[14] Li, X., Hagness, S.C., Choi, M.K., *et al.*: 'Numerical and experimental investigation of an ultrawideband ridged pyramidal horn antenna with curved launching plane for pulse radiation', *IEEE Antennas Wirel. Propag. Lett.*, 2003, **2**, (1), pp. 259–262

[15] Davidovits, J.: 'Geopolymers: inorganic polymeric new materials', *J. Therm. Anal.*, 1991, **37**, (8), pp. 1633–1656

[16] Pozar, D.M.: '*Microwave engineering*' (John Wiley and Sons Inc, Hoboken, NJ, USA, 2011, 4th Edn.)

[17] Andreev, Y.A., Kornienko, V.N., Liu, S.: 'Optimization of a combined high-power ultrawideband antenna', *J. Commun. Technol. Electron.*, 2017, **62**, (9), pp. 976–983

[18] Koshelev, V., *et al.*: 'High-power ultrawideband electromagnetic pulse radiation'. SPIE Proc, 1997, vol. 3158,

[19] Koshelev, V.I., Buyanov, Y.I., Andreev, Y.A., *et al.*: 'Ultrawideband radiators of high-power pulses PPPS-2001 pulsed power plasma science 2001'. 28th IEEE Int. Conf. on Plasma Science and 13th IEEE Int. Pulsed Power Conf.., Las Vegas, NV, USA, 2001, vol. 2, pp. 1661–1664

[20] Wang, S.F., Xie, Y.Z.: 'Design and optimization of high-power UWB combined antenna based on Klopfenstein impedance taper', *IEEE Trans. Antennas Propag.*, 2017, **65**, (12), pp. 6960–6967

[21] Lin, Z., Qiu, W., Pu, J., *et al.*: 'Accuracy and von Neumann stability of several highly accurate FDTD approaches for modelling Debye-type dielectric dispersion', *IET Microw Antennas Propag.*, 2018, **12**, (2), pp. 211–216

[22] Miller, P.: 'The measurement of antenna group delay'. The 8th European Conf. on Antennas and Propagation (EuCAP 2014), The Hague, The Netherlands, April 2014, pp. 1488–1492

[23] Essaidi, N., Nadir, H., Martinod, E., *et al.*: 'Comparative study of dielectric properties of geopolymer matrices using different dielectric powders', *J. Eur. Ceram. Soc.*, 2017, **37**, (11), pp. 3551–3557

[24] Jithin, D., Hussein, M.I., Awwad, F., *et al.*: 'Dielectric characterization of breast cancer cell lines using microwaves'. 2016 5th Int. Conf. on presented in Electronic Devices, Systems and Applications (ICEDSA), Ras Al Khaimah, United Arab Emirates, December 2016, pp. 1–4

[25] Shi, Y., Amert, A.K., Whites, K.W.: 'Miniaturization of ultrawideband monocone antennas using dielectric loading', *IEEE Trans. Antennas Propag.*, 2016, **64**, (2), pp. 432–441

[26] Ilarslan, M., Aydemir, M.E., Gose, E., *et al.*: 'The design and simulation of a compact Vivaldi shaped partially dielectric loaded (VS-PDL) TEM horn antenna for UWB applications'. 2013 IEEE Int. Conf. on Ultra-Wideband (ICUWB), Sydney, NSW, 2013, pp. 23–26

[27] Mohamed, H.A., Elsadek, H., Abdallah, E.A.F.: 'Design of compact DRH antenna for GPR transmitter application'. The 2nd Middle East Conf. on Antennas and Propagation, Cairo, 2012, pp. 1–4